Temperature dependence of the Kondo resonance in the photoemission spectra of the heavy-fermion compounds YbXCu$_4$ (X = Mg, Cd, and Sn)

Hiroaki Anzai [1,*] Kohei Morikawa,[1] Hiroto Shiono,[1] Hitoshi Sato,[2] Shin-ichiro Ideta,[3] Kiyohisa Tanaka,[3] Tao Zhuang,[4] Keisuke T. Matsumoto,[4] and Koichi Hiraoka[4,†]

[1]*Graduate School of Engineering, Osaka Prefecture University, Sakai 599-8531, Japan*
[2]*Hiroshima Synchrotron Radiation Center, Hiroshima University, Higashi-Hiroshima 739-0046, Japan*
[3]*UVSOR Synchrotron Facility, Institute for Molecular Science, Okazaki 444-8585, Japan*
[4]*Graduate School of Science and Engineering, Ehime University, Matsuyama, Ehime 790-8577, Japan*

We report a temperature-dependent study of Kondo resonance in the heavy-fermion compounds YbXCu$_4$ with X = Mg, Cd, and Sn. A sharp peak of the Yb^{2+} 4$f_{7/2}$ state has been observed in photoemission spectra, and its energy position in the limit of zero temperature is in agreement with the energy scale of the Kondo temperature T_K. The peak develops in the form of a dispersionless peak with large spectral weight at T_{coh} well below T_K. The onset temperature of the robust Kondo state is comparable to the temperature at a local maximum in magnetic susceptibility. This nontrivial development of changes in the Kondo resonance at T_{coh} demonstrates the formation of the coherent heavy-fermion state.

I. INTRODUCTION

In rare-earth compounds, the interaction between conduction electrons and localized-4f electrons (c–f hybridization) causes a loss in strength of the local magnetic moments and forms a correlated Fermi-liquid state with large effective electron mass at low temperatures. This heavy-fermion behavior is characterized by a resonant state near the Fermi energy (E_F). According to the single-impurity Anderson model, a sharp resonance peak in the electronic excitation spectrum appears at the energy scale of Kondo temperature T_K, which is a criterion for the magnetic response to a single magnetic impurity [1]. For ytterbium-based compounds, the spin-orbit split Yb^{2+} 4$f_{7/2}$ state is interpreted as the Kondo resonance state [2,3]. Its intensity is enhanced when the temperature varies from well above to well below T_K [4,5]. Therefore, studying the temperature dependence of the Kondo resonance over a wide temperature range will provide important insights for understanding the heavy-fermion state.

The periodic Anderson lattice model suggests a distinct temperature scale T_{coh}, which is associated with the onset of coherent screening at the lower temperatures and a criterion for the collective magnetic response to a lattice of local moments [6–8]. At temperatures above T_{coh}, the screening of a single local moment by conduction electrons is dominant. At temperatures $T < T_{coh}$, the collective screening results for coherent excitations of the heavy quasiparticles forms hybridized bands near E_F. Transport investigations have long provided evidence for the existence of T_{coh} in the Yb-based heavy-fermion systems. For example, the magnetic

susceptibility changes from Curie-Weiss behavior to being essentially independent of temperature at approximately T_{coh} [9,10]. It is generally accompanied by a drop in electrical resistivity, indicating the onset of coherence and the emergence of a Fermi-liquid behavior far below T_K [11,12]. Such a crossover towards the coherent states in the heavy-fermion systems has been rarely studied from microscopic measurements.

Photoemission spectroscopy is an excellent tool for studying the structure of single-particle excitations and allows direct observation of the characteristic resonant states in the heavy-fermion materials. We focus on the spectroscopic signature of YbXCu$_4$ (X = Mg, Cd, and Sn) with the same AuBe$_5$-type ($C15b$) crystal structure [10–13]. The compounds with X = Mg and Cd have large linear coefficients of specific heat $\sim$62 and $\sim$175 mJ K^{-2} mol^{-1}, respectively [11,12]. The fascinating property of YbXCu$_4$ is a variety of Kondo temperatures: T_K for X = Mg is approximately four times larger than T_K = 287 K for X = Cd [11,12]. In our previous report, the Kondo temperature for X = Sn was determined to be T_K = 503 K, indicating a strong hybridization of the Yb 4f states with the conduction bands [10]. The values of T_K are summarized in Table I. Coherent transport generally develops at well below T_K of the material [14]. Thus, the spectroscopic information at the experimentally accessible temperature of T_{coh} contributes to the understanding of the incoherent-coherent crossover in the heavy-fermion systems.

In this paper, we report the temperature dependence of the Kondo resonance in photoemission spectra of YbXCu$_4$ with X = Mg, Cd, and Sn. A sharp 4$f_{7/2}$ peak is observed clearly near E_F and exhibits a clear material dependence. Quantifying the energy position and spectral weight of the 4$f_{7/2}$ peak, we demonstrate the development of the coherent Kondo state in the form of a sharp and dispersionless peak at low

TABLE I. Characteristic temperatures in YbXCu$_4$ (X = Mg, Cd, and Sn). The Kondo temperature T_K is calculated by using the Wilson's formula $T_K = 1.29T_0$, where T_0 is the temperature scale determined from the susceptibility at zero temperature [15,16]. The values of T_0 and $\chi(0)$ are reported in Refs. [10–12]. The temperatures at the local maximum in the magnetic susceptibility T_χ^{max} for X = Cd and Sn are determined from $\chi(T)$ in Fig. 1(a). The value of T_χ^{max} for X = Mg is given in Refs. [11,12]. The onset temperatures T_{coh} are estimated from the temperature dependence of the Yb^{2+} $4f_{7/2}$ peak in Fig. 3(a).

X	T_K (K)	T_χ^{max} (K)	T_{coh} (K)
Mg	1109	130	122
Cd	287	35	60
Sn	503	40	59

temperatures much lower than T_K. This observation enabled us to obtain the consistent and reasonable spectroscopic data of the YbXCu$_4$ compounds.

High-quality single crystals of YbXCu$_4$ with X = Mg, Cd, and Sn were synthesized by the flux method [13]. The measurements of photoemission spectroscopy were performed on BL7U of the UVSOR Synchrotron Facility. The energy resolution was 16 meV. The data were collected with photon energy of $h\nu$ = 24 eV and in a wide temperature range below T_K of the samples. The samples were cleaved *in situ* and maintained under ultrahigh vacuum (8×10^{-9} Pa) during the measurements. Energies were calibrated with the Fermi edge of polycrystalline gold.

II. RESULTS AND DISCUSSION

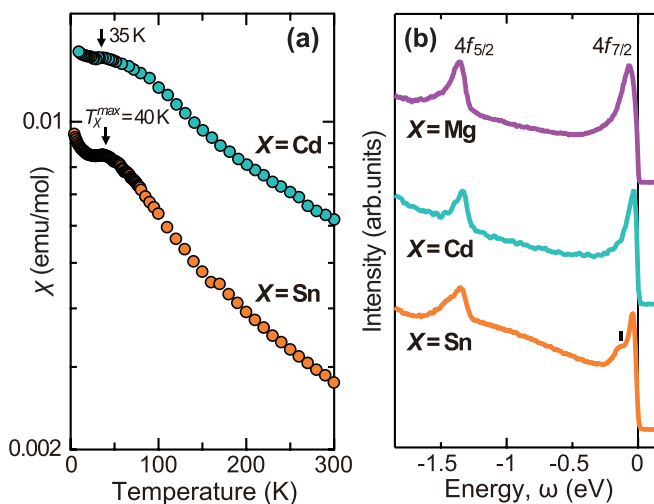Figure 1(a) shows the temperature dependences of the magnetic susceptibility $\chi(T)$ for X = Cd and Sn on a

logarithmic scale. The original data are reported in our previous publications [10,13]. The susceptibility deviates from the Curie-Weiss law with decreasing temperature and then exhibits a broad peak at low temperatures. A small upturn below 20 K may be due to the presence of impurity phases of Yb$_2$O$_3$ [13].

The ratio $\chi(T)/\chi(0)$ is a universal scaling with respect to T/T_0, where T_0 is the temperature scale deduced from the magnetic susceptibility at zero temperature within the Coqblin-Schrieffer model [15,16]. For the data in Fig. 1(a), it is difficult to determine $\chi(0)$ due to the upturn at $T < 20$ K. Here, we estimated the temperature at the local maximum T_χ^{max} as a characteristic temperature. The temperature is indicated by arrows in Fig. 1(a) and summarized in Table I. The value for X = Mg has been reported in the literature [11,12]. We note that the weak peak in $\chi(T)$ for X = Cd causes large error bars in T_χ^{max}. It is revealed that T_K is proportional to T_χ^{max} by a factor of $\sim$9.5.

In Fig. 1(b), the photoemission spectra of YbXCu$_4$ measured at T = 8 K are presented. The spectra consist of a spin-orbit doublet of the Yb^{2+} $4f$ states: the $4f_{5/2}$ and $4f_{7/2}$ states are peaked at $|\omega| \simeq 1.35$ eV and near E_F, respectively. These assignments are in agreement with the previous photoemission studies [17–20]. The full energy width at half maximum 0.107 eV of the $4f_{7/2}$ peak for X = Mg is much narrower than the results obtained by using a He discharge lamp [17], indicating the high-quality data in this paper.

A shoulder structure is seen at the high-energy side of the $4f_{7/2}$ peak as indicated by the vertical bar in the spectra of X = Sn. The relative intensity and energy difference coincide well with the those of the spin-orbit partner of the $4f_{5/2}$ state, suggesting the $4f$-derived electronic states. A similar structure has been observed in the spin-orbit split states of YbInCu$_4$ [18,19]. For the case of X = Mg and Cd, the $4f_{5/2}$ and $4f_{7/2}$ peaks exhibit an asymmetric line shape. We consider that a shoulder of the $4f_{7/2}$ peak also exists in the spectra of X = Mg and Cd, but its small spectral weight may be smeared due to the high-energy tail of the main peak and the limitation of the experimental energy resolution.

A candidate for the origin of the shoulder structure is the $4f$ states of the subsurface region that intervenes between the surface and the bulk regions of the crystal [18–21]. The electronic state of the subsurface region exhibits characteristics intermediate between those at the surface and those in the bulk [21]. The observed shoulder is, indeed, located between the surface-derived state at $|\omega| \simeq 1.1$ eV and the bulk-derived $4f_{7/2}$ state near E_F [20]. It is, therefore, reasonable to assign the shoulder of the $4f_{7/2}$ peak to the $4f$-derived states in the Yb subsurface atomic layers.

The temperature dependences of the $4f_{7/2}$ peak for X = Mg, Cd, and Sn, respectively, are shown in Figs. 2(a)–2(c). The peaks at T = 8 K are located away from the energy width of the thermal broadening $4k_BT$ in the neighborhood of E_F, where k_B is Boltzmann's constant. Therefore, we can rule out the possibility that the intense peak near E_F, such as the Kondo resonance in the Ce compounds, is observed due to the cutoff of the Fermi-Dirac function [22]. The enhancement of the peak intensity with decreasing temperature is essentially consistent with the predictions of the Anderson impurity model [1].
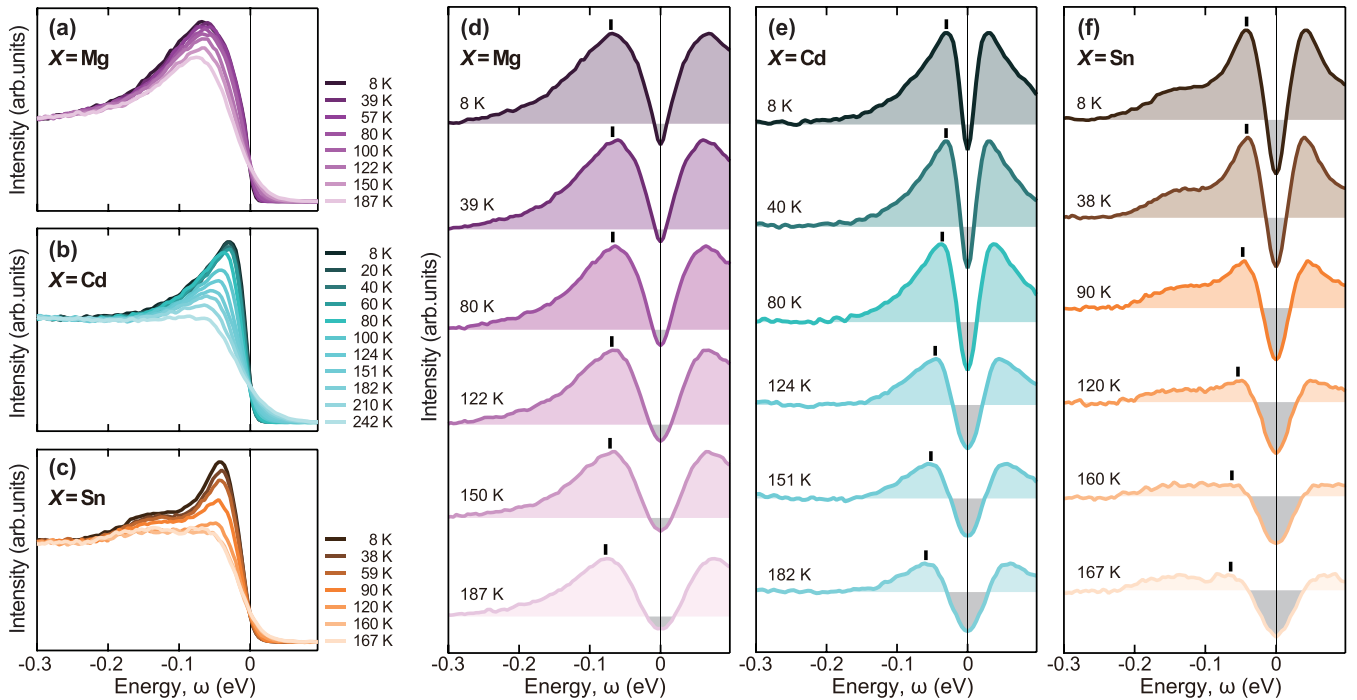

FIG. 1. (a) Temperature dependence of magnetic susceptibility $\chi(T)$ for YbXCu$_4$ with X = Cd and Sn. The original data are reported in Refs. [10,13]. Arrows represent temperatures at the local maximum in $\chi(T)$. (b) The photoemission spectra of YbXCu$_4$ measured at T = 8 K. The vertical bar indicates the characteristic energy state.

FIG. 2. (a) Temperature dependence of the Yb^{2+} $4f_{7/2}$ peak in photoemission spectra for $X = Mg$. The spectra are normalized to the intensity at $|\omega| \simeq 0.3$ eV. (b) and (c) The same spectra as in panel (a) but for (b) $X = Cd$ and (c) $X = Sn$. (d) Temperature dependence of the symmetrized spectra for $X = Mg$. The spectra at six characteristic temperatures are selected from panel (a). An offset is used for clarity. (e) and (f) The same spectra as in panel (d) but for (e) $X = Cd$ and (f) $X = Sn$. The vertical bars denote the energy positions of the $4f_{7/2}$ peak. The colored area indicates the low-energy spectral weight W_{LE}. The area in the neighborhood of E_F is also shaded in gray.

A key finding from the raw spectra is a distinct temperature evolution of the $4f_{7/2}$ peak. The peak intensity of $X = Cd$ and Sn decreases rapidly with increasing temperature. The intensity of $X = Mg$, however, is maintained even at the high temperature of $T \simeq 190$ K. Furthermore, the peak positions of $X = Mg$ are less sensitive to temperature compared with those of $X = Cd$ and Sn as shown in Figs. 2(a)–2(c). This is consistent with the robustness of the Kondo singlet state in $X = Mg$, where T_K is larger than that of $X = Cd$ and Sn.

To quantify the energy and intensity of the $4f_{7/2}$ peak precisely, we have symmetrized the photoemission spectra with respect to E_F. This method can remove the effects of the Fermi-Dirac cutoff on spectra near E_F and provides a clear view of temperature dependence of the photoemission spectra [23]. The symmetrized spectra are shown with a constant offset in Figs. 2(d)–2(f). We have determined the energy positions of the peak and plotted them as a function of temperature in Fig. 3(a), which reveals a universal trend in YbXCu$_4$. The peak energy of $X = Mg$ decreases with decreasing temperature from $T = 187$ to 122 K and then saturates at low temperatures. The similar saturation is seen in the results for $X = Cd$ and Sn.

It is noteworthy that the onset temperatures, which start to approach saturation, are comparable to T_χ^{max} shown in Fig. 1(a) and Table I. The consistency of the spectroscopic data with the magnetic susceptibility data indicates that the dispersionless feature of the $4f_{7/2}$ peak at low temperatures is relevant to the coherent excitations of the heavy quasiparticles below T_{coh}. We have estimated the onset temperatures of the peak saturation as T_{coh} and summarized them in Table I.

The appearance of the Kondo resonance at $k_B T_K$ in the limit of zero temperature represents the formation of the Kondo singlet state [4]. In this context, we have applied the average of the peak energy over the region of the saturation to the energy scale of the Kondo temperature. As shown by the dashed line in Fig. 3(a), the average energies for $X = Mg$, Cd, and Sn are determined to be approximately 69, 30, and 42 meV, respectively. These energy scales are in agreement with the sample's T_K shown in Table I. Therefore, the observed $4f_{7/2}$ state is responsible for the heavy-fermion behavior of YbXCu$_4$.

The intensity of the Kondo resonance indicates the strength of the c–f hybridization [4,5]. We have checked the temperature dependence of the spectral weight at low energies. As shown in Figs. 2(a)–2(c), the line shape near $|\omega| \simeq 0.3$ eV is identical within the noise level. Thus, we have subtracted the constant intensity at ∼0.3 eV from each spectrum and displayed them as colored areas in Figs. 2(d)–2(f). The spectral weights for $X = Cd$ and Sn are rapidly suppressed with increasing temperature. In contrast, the spectral weight for $X = Mg$ remains largely unchanged even at $T \simeq 190$ K. These results indicate the robustness of the Kondo state in YbMgCu$_4$.

In the research of high-T_c superconductors, a decrease in the dip minimum intensity at E_F is interpreted as an increase in the energy gap in the neighborhood of E_F [23,24]. For the spectra of YbXCu$_4$ in Figs. 2(d)–2(f), the $4f_{7/2}$ peak shifts to higher energy with keeping the same dip minimum, demonstrating no gap opening at E_F. Previous Hall effect measurements, indeed, reveal metallic behaviors of the YbXCu$_4$ compounds with a healthy density of states [25]. Therefore,
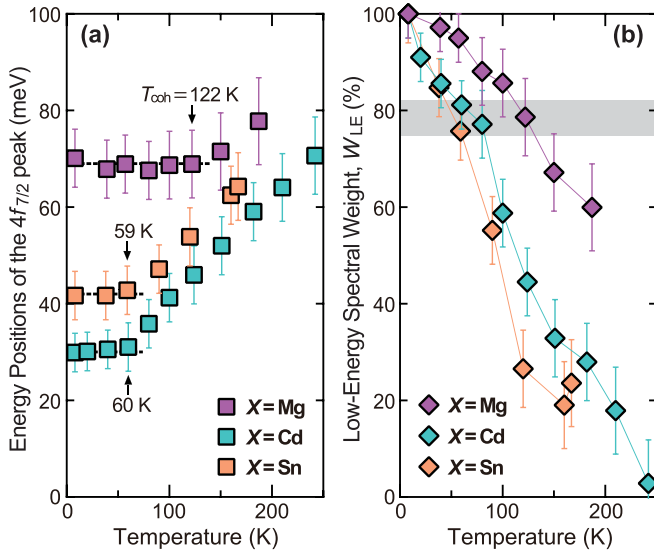
FIG. 3. (a) Temperature dependence of energy positions of the Yb^{2+} $4f_{7/2}$ peak. The arrows represent the onset temperature for the saturation of peak energy. The dashed lines indicate the average of the peak energy over the region of the saturation. (b) Temperature dependence of low-energy spectral weight W_{LE}, which is determined by the integration of peak intensity over the colored area of the symmetrized spectra in Figs. 2(d)–2(f). The weight is plotted as a percentage of the total weight at $T = 8$ K. The shaded area indicates the crossover region in W_{LE}. The error bars derived from statistical and reflected by noise in the data.

the characteristic dip in the symmetrized spectra is indicative of the shift in energy of the Kondo resonance.

The low-energy spectral weight W_{LE} is determined by integrating the peak intensity over the energy window of the colored areas in Figs. 2(d)–2(f). This method is simple and reasonable for extracting W_{LE} from different samples with different types of spectral shapes [26]. Another method for the background subtraction and its consistency are discussed in Appendix A. Figure 3(b) shows the temperature dependence of W_{LE} as a percentage of the total weight at $T = 8$ K. We note that W_{LE} for $X = $ Sn reflects mainly the development of the $4f_{7/2}$ peak because the background-subtracted intensity of the shoulder structure is insensitive to temperature. As temperature increases, W_{LE} for $X = $ Cd and Sn rapidly decreases and is less than 30% at $T \simeq 150$ K. For $X = $ Mg, in contrast, the weight of 65% persists at the same temperature. These results suggest strong hybridization of the $4f$ electrons with the conduction electrons in $YbMgCu_4$ [10,11].

The rate of decrease in W_{LE} changes at $\sim 78\%$ as indicated by the gray-shaded area in Fig. 3(b). The ratio is quantitatively similar to the temperature region where the saturation of the peak energy occurs in Fig. 3(a). Therefore, these remarkable changes in the Kondo resonance demonstrate the emergence of a crossover between the two regimes of Kondo screening at the higher scale and coherent screening at the lower scale. The crossover temperature is considered to be T_{coh} shown in Fig. 3(a) and Table I. The two relevant energy scales of T_{coh} and T_K in the heavy-fermion compounds are consistent with the protracted screening behavior predicted by the periodic Anderson lattice model [6,7].

We next discuss the electronic band structure near E_F. The crystal-field splitting of $4f$ states in $YbRh_2Si_2$ has been observed by angle-resolved photoemission spectroscopy [27]. The hybridization of the $4f$ states with the conduction band locally deforms the band structure at their crossing point in momentum space [27–31]. Thus far, the energy dispersion of the crystal-field-split $4f$ states as well as that of the conduction bands has not been observed in $YbXCu_4$. The eightfold degenerate Hunds rule ground state of Yb^{3+} with $J = 7/2$ splits into two Kramers doublets and one quartet in the cubic site symmetry of the $C15b$ structure [32]. The overall splitting energy is estimated to be ~ 8 meV [33,34]. This value is within the error bars of the data in Fig. 3(a). Even though the low-energy and high-energy tails of the $4f_{7/2}$ peak in Fig. 2 may be related to the energy dispersion of the conduction bands, the observed $4f_{7/2}$ peak in the momentum-integrated spectra reflects the essential features of the Kondo resonance.

Under these circumstances, the Kondo resonance develops in the form of a sharp and dispersionless peak below T_{coh} as demonstrated by the peak position and spectral weight in Fig. 3. Moreover, we have confirmed the consistency of the peak width of $X = $ Cd in Appendix B. Such an evolution of the Kondo resonance indicates the formation of coherent heavy quasiparticle bands, which are accompanied by the opening of a hybridization gap at the crossing point of the conduction and $4f$ bands [27–31]. We assume a reconstruction of the Fermi surface at T_{coh} of $YbXCu_4$, such as the change from small to large Fermi surfaces with increasing the strength of c–f hybridization [28–30]. The Fermi surfaces and their orbital characters are key ingredients for understanding the low-energy physics. Further investigations, such as angle-resolved photoemission spectroscopy measurements are required to fully describe the electronic band structure of $YbXCu_4$.

III. CONCLUSION

We have revealed the temperature dependence of the Kondo resonance in the heavy-fermion compound $YbXCu_4$ by synchrotron radiation photoemission spectroscopy. The intense peak of the Yb^{2+} $4f_{7/2}$ state is observed near E_F in all spectra. The $4f_{7/2}$ peak shifts closer to E_F and becomes sharper with decreasing temperature. Below T_{coh}, the peak with a large spectral weight does not show temperature dependence. The peak positions in the limit of zero temperature are quantitatively consistent with the energy scales of Kondo temperature, demonstrating that the observed $4f_{7/2}$ peak is certainly the Kondo resonance in $YbXCu_4$. It is interesting to note that T_{coh} is comparable with the crossover temperature T_χ^{max} to the ground-state Fermi liquid with coherent transport. Our results suggest the development of the coherent heavy-fermion state below T_{coh}.
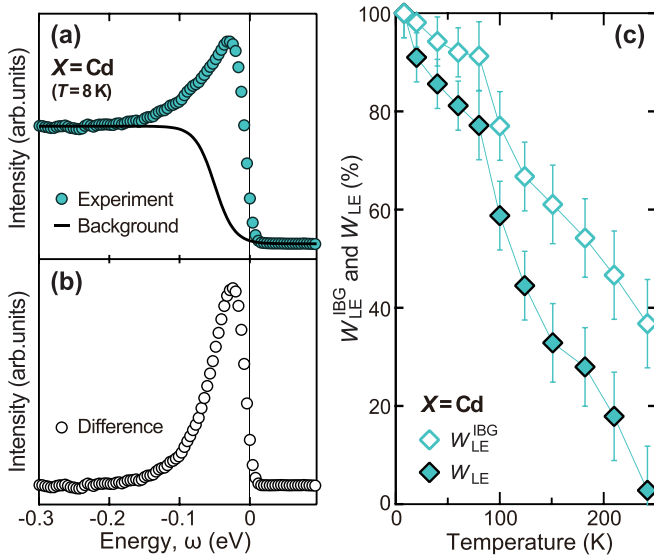
FIG. 4. (a) The Yb^{2+} $4f_{7/2}$ peak in the photoemission spectra of $X = Cd$ is taken from the original data of Fig. 2(b). The black curve represents the temperature-independent integral-type background. (b) The difference spectra between the raw data and the background in panel (a). (c) Comparison of the low-energy spectral weight obtained by two different methods for background subtraction. The open diamonds represent the results extracted from the subtraction of the integral-type background W_{LE}^{IBG}. The same data of W_{LE} for $X = Cd$ in Fig. 3(b) are shown as filled diamonds.

APPENDIX A: BACKGROUND SUBTRACTION

In Appendix A, we compare the low-energy spectral weight W_{LE} with that obtained by another method for the background subtraction. Figure 4(a) shows again the $4f_{7/2}$ peak in the photoemission spectra of $X = Cd$ at $T = 8$ K. Here, we adopted the temperature-independent integral-type background (IBG) for extracting W_{LE}^{IBG} and plotted it as the black curve [35]. This method is widely used for the evaluation of the photoemission spectra [17,18,20,21]. The difference between the raw data and the background is depicted by the open circles in Fig. 4(b). The high-energy tail of the difference spectra may be derived from the energy dispersion of the conduction band as discussed in the main text.

We integrated the intensity of the difference spectra over an energy window of $0 \leqslant |\omega| \leqslant 0.3$ eV and then normalized the spectral weight as a percentage of the total weight at $T = 8$ K. The temperature dependence of W_{LE}^{IBG} is shown by the open diamonds in Fig. 4(c) together with W_{LE} extracted from the subtraction of the constant background. One clearly sees that the rate of decrease in W_{LE}^{IBG} and W_{LE} changes at the same temperature. This consistency demonstrates that the choice of background subtraction does not affect the results of our analysis.

APPENDIX B: PEAK WIDTH

We now examine the peak width of the $4f_{7/2}$ state as a function of temperature. Figure 5(a) shows the
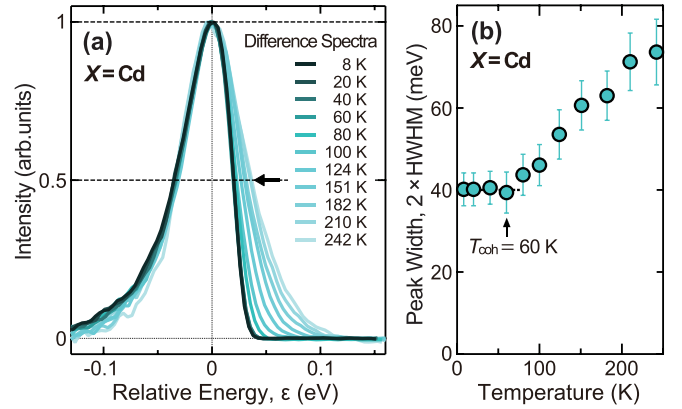

FIG. 5. (a) Temperature evolution of peak width for $X = Cd$ plotted on a relative energy scale ε. The intensity of difference spectra is normalized to the highest intensity of each spectrum. The energy position of spectral midpoint, defined as energies where the spectral peaks become half in intensity, is shown by the arrow. (b) Temperature dependence of peak width $2 \times$ HWHM. The HWHM is determined by the half width at half maximum in the low-energy region ($\varepsilon \geqslant 0$ eV). The arrow indicates the onset temperature for the saturation of the peak width. The dashed line represents the average of the peak width over the region of the saturation.

difference spectra of $X = Cd$ plotted on a relative energy scale ε with respect to the $4f_{7/2}$ peak. The intensity is normalized to the highest intensity of each spectrum. The spectra in the high-energy region ($\varepsilon < 0$ eV) have an almost identical shape. On the other hand, the spectra in the low-energy region ($\varepsilon \geqslant 0$ eV) exhibit a clear temperature dependence: The energy position of spectral midpoint rapidly shifts above $T \simeq 60$ K as shown by an arrow in Fig. 5(a).

We have determined the peak width by using the half width at half maximum (HWHM) in the low-energy region because the full width at half maximum does not yield the correct width due to the asymmetric line shape. The peak width $2 \times$ HWHM is plotted in Fig. 5(b) as a function of temperature. The width decreases with decreasing temperature from $T = 242$ to 60 K and then saturates at low temperatures. This trend is in good agreement with the temperature dependence of the energy position of the $4f_{7/2}$ peak in Fig. 3(a). The average of the peak width over the region of the saturation is estimated to be 40 meV, which is comparable to or larger than the energy scale of $T_K = 287$ K for $X = Cd$.

The experimental and thermal broadenings have a non-negligible effect on the width of the Kondo resonance [36]. Moreover, the effect of a repulsive term describing $d-f$ Coulomb interaction and the scattering processes of photoelectrons to phonons or electron-hole excitations make a broadening of spectral features [36,37]. We emphasize here that the development of the Kondo resonance at T_{coh} is not only evident from the peak position and spectral weight in Fig. 3, but also evident from the peak width in Fig. 5.

[1] R. I. R. Blyth, J. J. Joyce, A. J. Arko, P. C. Canfield, A. B. Andrews, Z. Fisk, J. D. Thompson, R. J. Bartlett, P. Riseborough, J. Tang, and J. M. Lawrence, Temperature-invariant valence-band $4f$ photoemission features in the heavy-fermion compound $YbAl_3$, Phys. Rev. B **48**, 9497 (1993).

[2] L. H. Tjeng, S.-J. Oh, E.-J. Cho, H.-J. Lin, C. T. Chen, G.-H. Gweon, J.-H. Park, J. W. Allen, T. Suzuki, M. S. Makivić, and D. L. Cox, Temperature Dependence of the Kondo Resonance in $YbAl_3$, Phys. Rev. Lett. **71**, 1419 (1993).

[3] P. Weibel, M. Grioni, D. Malterre, B. Dardel, Y. Baer, M. J. Besnus, Temperature dependence of the Kondo peak in photoemission spectra of $YbAgCu_4$, Z. Phys. B **91**, 337 (1993).

[4] N. E. Bickers, D. L. Cox, and J. W. Wilkins, Self-consistent large-N expansion for normal-state properties of dilute magnetic alloys, Phys. Rev. B **36**, 2036 (1987).

[5] F. Patthey, J.-M. Imer, W.-D. Schneider, H. Beck, Y. Baer, and B. Delley, High-resolution photoemission study of the low-energy excitations in $4f$-electron systems, Phys. Rev. B **42**, 8864 (1990).

[6] P. Nozières, Impuretès magnètiques et effet Kondo, Ann. Phys. (Paris) **10**, 19 (1985).

[7] A. N. Tahvildar-Zadeh, M. Jarrell, and J. K. Freericks, Low-Temperature Coherence in the Periodic Anderson Model: Predictions for Photoemission of Heavy Fermions, Phys. Rev. Lett. **80**, 5168 (1998).

[8] Y.-F. Yang, Z. Fisk, H.-O. Lee, J. D. Thompson, and D. Pines, Scaling the Kondo lattice, Nature (London) **454**, 611 (2008).

[9] S. Friedemann, T. Westerkamp, M. Brando, N. Oeschler, S. Wirth, P. Gegenwart, C. Krellner, C. Geibel, and F. Steglich, Detaching the antiferromagnetic quantum critical point from the Fermi-surface reconstruction in $YbRh_2Si_2$, Nat. Phys. **5**, 465 (2009).

[10] H. Anzai, S. Ishihara, H. Shiono, K. Morikawa, T. Iwazumi, H. Sato, T. Zhuang, K. T. Matsumoto, and K. Hiraoka, Mixed-valence state of the rare-earth compounds $YbXCu_4$ (X = Mg, Cd, In, and Sn): Magnetic susceptibility, x-ray diffraction, and x-ray absorption spectroscopy investigations, Phys. Rev. B **100**, 245124 (2019).

[11] J. L. Sarrao, C. D. Immer, Z. Fisk, C. H. Booth, E. Figueroa, J. M. Lawrence, R. Modler, A. L. Cornelius, M. F. Hundley, G. H. Kwei, J. D. Thompson and F. Bridges, Physical properties of $YbXCu_4$ (X = Ag, Au, Cd, Mg, Tl, and Zn) compounds, Phys. Rev. B **59**, 6855 (1999).

[12] T. Koyama, M. Matsumoto, T. Tanaka, H. Ishida, T. Mito, and S. Wada, Physical properties of the Kondo compounds $YbXCu_4$ (X = Au, Ag, In, Cd, Tl, and Mg) probed by ^{63}Cu NMR, Phys. Rev. B **66**, 014420 (2002).

[13] K. Hiraoka, K. Kojima, T. Hihara, and T. Shinohara, NMR study of $YbCdCu_4$ and $YbTlCu_4$, J. Magn. Magn. Mater. **140-144**, 1243 (1995).

[14] M. F. Hundley, P. C. Canfield, J. D. Thompson, Z. Fisk, and J. M. Lawrence, Hybridization gap in $Ce_3Bi_4Pt_3$, Phys. Rev. B **42**, 6842 (1990).

[15] V. T. Rajan, Magnetic Susceptibility and Specific Heat of the Coqblin-Schrieffer Model, Phys. Rev. Lett. **51**, 308 (1983).

[16] N. Andrei and J. H. Lowenstein, Scales and Scaling in the Kondo Model, Phys. Rev. Lett. **46**, 356 (1981).

[17] H. Sato, K. Hiraoka, M. Taniguchi, Y. Takeda, M. Arita, K. Shimada, H. Namatame, A. Kimura, K. Kojima, T. Muro, Y. Saitoh, A. Sekiyama, and S. Suga, Electronic structure of $YbXCu_4$ (X = In, Cd, Mg) investigated by high-resolution photoemission spectroscopy, J. Synchrotron Radiat. **9**, 229 (2002).

[18] H. Sato, K. Yoshikawa, K. Hitaoka, M. Arita, K. Fujimoto, K. Kojima, T. Muro, Y. Saitoh, A. Sekiyama, S. Suga, and M. Taniguchi, Soft-x-ray high-resolution photoemission study on the valence transitions in $YbInCu_4$, Phys. Rev. B **69**, 165101 (2004).

[19] S. Ishihara, K. Ichiki, K. Abe, T. Matsumoto, K. Mimura, H. Sato, M. Arita, Eike F. Schwier, H. Iwasawa, K. Shimada, H. Namatame, M. Taniguchi, T. Zhuang, and K. Hiraoka, The c-f hybridization effect in the subsurface region of $YbInCu_4$, J. Electron Spectrosc. Relat. Phenom. **220**, 66 (2017).

[20] F. Reinert, R. Claessen, G. Nicolay, D. Ehm, S. Hüfner, W. P. Ellis, G.-H. Gweon, J. W. Allen, B. Kindler, and W. Assmus, Photoemission experiments on $YbInCu_4$: Surface effects and temperature dependence, Phys. Rev. B **58**, 12808 (1998).

[21] S. Suga, A. Sekiyama, S. Imada, J. Yamaguchi, A. Shigemoto, A. Irizawa, K. Yoshimura, M. Yabashi, K. Tamasaku, A. Higashiya, and T. Ishikawa, Unraveling genuine first order bulk valence transition and kondo resonance behaviors in $YbInCu_4$ by high energy photoelectron spectroscopy, J. Phys. Soc. Jpn. **78**, 074704 (2009).

[22] D. Ehm, S. Hüfner, F. Reinert, J. Kroha, P. Wölfle, O. Stockert, C. Geibel, H. v. Löhneysen, Phys. Rev. B **76**, 045117 (2007).

[23] M. R. Norman, Destruction of the Fermi surface in underdoped high-Tc superconductors, Nature (London) **392**, 157 (1998).

[24] H. Anzai, A. Ino, M. Arita, H. Namatame, M. Taniguchi, M. Ishikado, K. Fujita, S. Ishida, and S. Uchida, Relation between the nodal and antinodal gap and critical temperature in superconducting Bi2212, Nat. Commun. **4**, 1815 (2013).

[25] E. Figueroa, J. M. Lawrence, J. L. Sarrao, Z. Fisk, M. F. Hundley, and J. D. Thompson, Hall effect in $YbXCu_4$ and the role of carrier density in the $YbInCu_4$ valence transition, Solid State Commun. **106**, 347 (1998).

[26] T. Kondo, R. Khasanov, T. Takeuchi, J. Schmalian, and A. Kaminski, Competition between the pseudogap and superconductivity in the high-T_c copper oxides, Nature (London) **457**, 296 (2009).

[27] D. V. Vyalikh, S. Danzenbächer, Y. Kucherenko, K. Kummer, C. Krellner, C. Geibel, M. G. Holder, T. K. Kim, C. Laubschat, M. Shi, L. Patthey, R. Follath, and S. L. Molodtsov, k Dependence of the Crystal-Field Splittings of $4f$ States in Rare-Earth Systems, Phys. Rev. Lett. **105**, 237601 (2010).

[28] H. C. Choi, K. Haule, G. Kotliar, B. I. Min, and J. H. Shim, Observation of a kink during the formation of the Kondo resonance band in a heavy-fermion system, Phys. Rev. B **88**, 125111 (2013).

[29] S. Jang, J. D. Denlinger, J. W. Allen, V. S. Zapf, M. B. Maple, J. N. Kim, B. G. Jang, and J. H. Shim, Evolution of the Kondo lattice electronic structure above the transport coherence temperature, arXiv:1704.08247.

[30] Q. Y. Chen, D. F. Xu, X. H. Niu, J. Jiang, R. Peng, H. C. Xu, C. H. P. Wen, Z. F. Ding, K. Huang, L. Shu, Y. J. Zhang, H. Lee, V. N. Strocov, M. Shi, F. Bisti, T. Schmitt, Y. B. Huang, P. Dudin, X. C. Lai, S. Kirchner, H. Q. Yuan, and D. L. Feng, Direct observation of how the heavy-fermion state develops in $CeCoIn_5$, Phys. Rev. B **96**, 045107 (2017).

[31] J. Hwang, K. Kim, H. Ryu, J. Kim, J.-E. Lee, S. Kim, M. Kang, B.-G. Park, A. Lanzara, J. Chung, S.-K. Mo,

J. Denlinger, B. I. Min, and C. Hwang, Emergence of kondo resonance in graphene intercalated with cerium, Nano Lett. **18**, 3661 (2018).

[32] T. Willers, J. C. Cezar, N. B. Brookes, Z. Hu, F. Strigari, P. Körner, N. Hollmann, D. Schmitz, A. Bianchi, Z. Fisk, A. Tanaka, L. H. Tjeng, and A. Severing, Magnetic Field Induced Orbital Polarization in Cubic YbInNi$_4$: Determining the Quartet Ground State Using X-Ray Linear Dichroism, Phys. Rev. Lett. **107**, 236402 (2011).

[33] G. Polatsek and P. Bonville, Interpretation of neutron magnetic scattering in the Kondo lattices YbPd$_2$Si$_2$ and YbAgCu$_4$, Z. Phys. B **88**, 189 (1992).

[34] P. G. Pagliuso, J. D. Thompson, J. L. Sarrao, M. S. Sercheli, C. Rettori, G. B. Martins, Z. Fisk, and S. B. Oseroff, Crystal field study in rare-earth-doped LuInNi$_4$, Phys. Rev. B **63**, 144430 (2001).

[35] D. A. Shirley, High-resolution x-ray photoemission spectrum of the valence bands of gold, Phys. Rev. B **5**, 4709 (1972).

[36] S. Hüfner, *Photoelectron Spectroscopy*, 2nd ed., Springer Series in Solid-State Sciences Vol. 82 (Springer-Verlag, Berlin/Heidelberg/New York, 1996).

[37] M. Takeshige, O. Sakai, and T. Kasuya, $4f$-band of Ce-compounds in photoexcitation and in low energy phenomena, J. Magn. Magn. Mater. **52**, 363 (1985).